

Metamagnetic ripples in the UTe_2 high magnetic field phase diagram

Zheyu Wu,¹ Hanyi Chen,¹ Mengmeng Long,¹ Gangjian Jin,² Huakun Zuo,² Daniel Shaffer,³
Dmitry V. Chichinadze,⁴ Andrej Cabala,⁵ Vladimír Sechovský,⁵ Michal Vališka,⁵
Zengwei Zhu,² Gilbert G. Lonzarich,¹ F. Malte Grosche,¹ and Alexander G. Eaton^{1,*}

¹*Cavendish Laboratory, University of Cambridge,*

JJ Thomson Avenue, Cambridge, CB3 0HE, United Kingdom

²*Wuhan National High Magnetic Field Center, Wuhan 430074, China*

³*Department of Physics, University of Wisconsin-Madison, Madison, Wisconsin 53706, USA*

⁴*National High Magnetic Field Laboratory, Tallahassee, Florida, 32310, USA*

⁵*Charles University, Faculty of Mathematics and Physics,*

Department of Condensed Matter Physics, Ke Karlovu 5, Prague 2, 121 16, Czech Republic

(Dated: March 17, 2025)

The heavy fermion metamagnet uranium ditelluride possesses two distinct magnetic field-induced superconducting states. One of these superconductive phases resides at magnetic fields immediately below a first-order metamagnetic transition to a field-polarized paramagnetic state at a field strength H_m , while the other exists predominantly above H_m . However, little is known about the microscopic properties of this polarized paramagnetic state. Here we report pulsed magnetic field measurements tracking the evolution of H_m for polar and azimuthal inclinations in the vicinity of the crystallographic b - a plane. We uncover a region of the phase diagram at high fields > 50 T with a ripple-like non-monotonic dependence of H_m on the orientation of field. Within this ripple in the metamagnetic transition surface, H_m exhibits an anomalous temperature dependence. Our results point towards the presence of complex magnetic interactions and possible magnetic sub-phases at high magnetic fields in UTe_2 , which may have important implications for the manifestation of exotic field-induced superconductivity.

The actinoid dichalcogenide UTe_2 is a promising candidate for realizing multi-phase odd-parity superconductivity [1, 2]. This compound crystallizes in a body-centred orthorhombic structure (space group 71) with $Immm$ symmetry [3]. At ambient pressure, three distinct superconducting phases have been observed for various inclinations of applied magnetic field \mathbf{H} up to the remarkably high scale of $\mu_0 H \approx 70$ T [1, 2, 4–13] for temperature $T < 2.1$ K. Evidence favoring the scenario of odd-parity pairing stems chiefly from high critical fields that exceed the Pauli-Chandrasekhar-Clogston limit for all orientations of \mathbf{H} [8, 14, 15], along with only small changes in the Knight shift on crossing the superconducting critical temperature T_c as measured by nuclear magnetic resonance (NMR) [16–18].

For \mathbf{H} oriented along the crystallographic b -axis – the hard magnetic direction of UTe_2 – superconductivity persists at low temperatures up to $\mu_0 H \approx 34$ T, whereat it is abruptly truncated by a first-order metamagnetic transition to a polarized paramagnetic state [5, 6]. There is strong evidence indicating that the superconductivity observed at $\mu_0 H \gtrsim 15$ T constitutes a distinct thermodynamic phase from that at lower H [7, 19]. As the orientation of \mathbf{H} is rotated away from b the metamagnetic transition field H_m has been reported to increase monotonically [4]. For a narrow angular range of \mathbf{H} , yet another superconductive state has been observed at $H > H_m$ [5]. Initially discovered for rotations from b towards c – where it typically starts at $\mu_0 H \approx 40$ T

and extends up to around 70 T – recent measurements have indicated that this remarkable field-induced superconductive state occupies an extended three-dimensional section of magnetic field space, encircling the b -axis in a toroidal shape [11, 12]. At its zenith it exhibits a higher T_c for $\mu_0 H > 40$ T than it does at $\mu_0 H = 0$ T [13]. Magnetoconductance measurements to very high H have indicated that this torus of highly field-resilient superconductivity is anchored to a quantum critical phase boundary demarcating polarized paramagnetism from the normal paramagnetic state [12]. Deciphering the intimate connection between the metamagnetic phase transition and the field-induced superconducting phases is one of the central challenges in understanding the exotic physical properties of UTe_2 .

The extent of the high- H superconductivity in the b - c plane has been extensively probed by numerous studies [4, 5, 9, 10, 13, 21–23]. For \mathbf{H} tilted out of the b - c plane towards the a direction, the onset field of high- H superconductivity has been reported to track the rise in H_m , and its extent has been proposed to extend up to very high values of H [11]. However, few studies have mapped the geometry of the metamagnetic transition surface for large H_a magnetic field components. Given the intimate connection between the metamagnetic transition and the intriguing field-induced superconducting phases of UTe_2 – one of which terminates at H_m , while another exists above H_m – a detailed understanding of the evolution of H_m as a function of magnetic field orientation is necessary to better understand the manifestation of exotic \mathbf{H} -induced superconductivity in UTe_2 .

Prior high field measurements have indicated that H_m

* alex.eaton@phy.cam.ac.uk

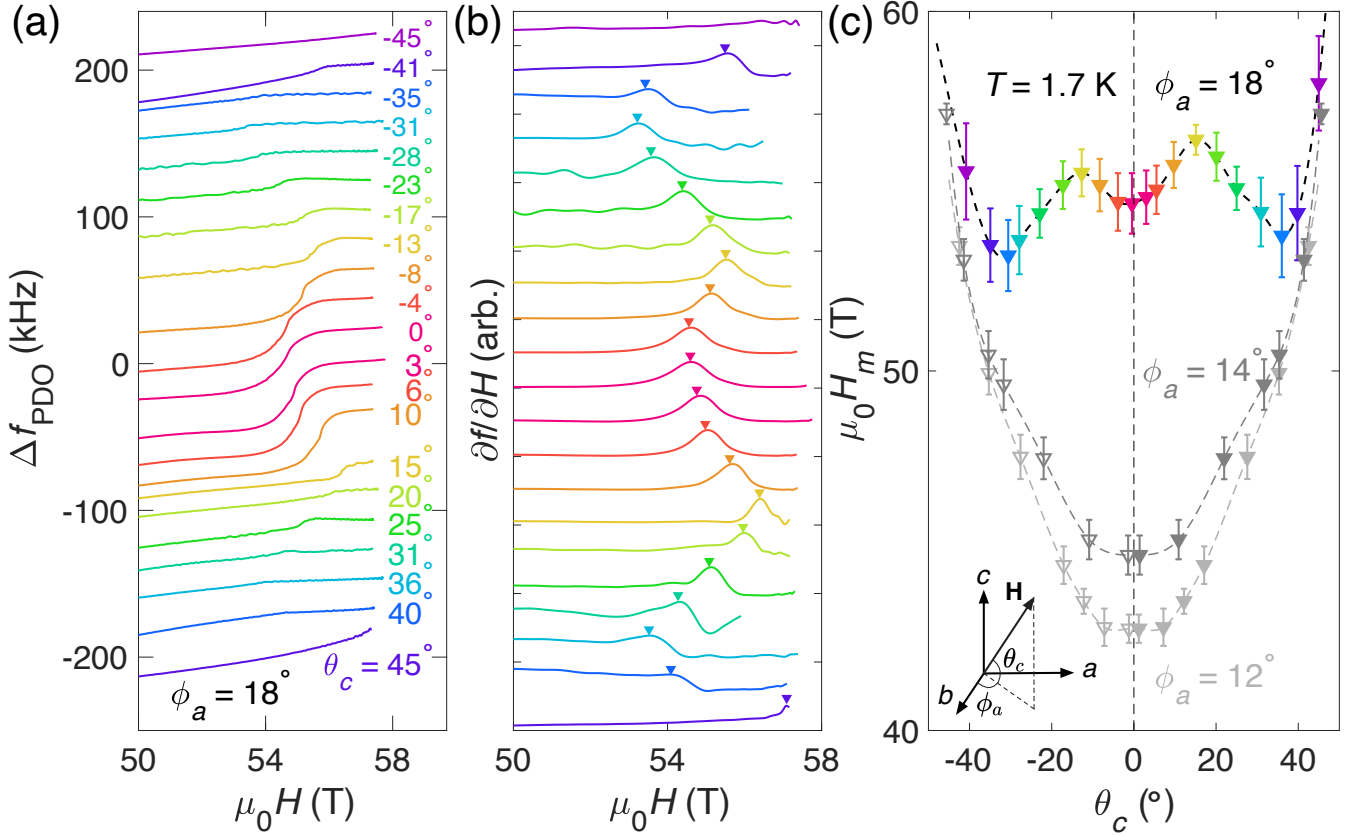


FIG. 1. Non-monotonic angular evolution of H_m . (a) Contactless conductivity measured by the PDO technique in pulsed magnetic fields of strength H at temperature $T = 1.7$ K. The sample was fixed at an azimuthal inclination of $\phi_a = 18^\circ$ and rotated through positive and negative values of the polar angle θ_c up to $|\theta_c| = 45^\circ$. (b) Derivative with respect to H of the contactless conductivity data in panel (a). Markers identify the location of H_m for each curve, defined as the peak in the derivative of the signal. Curves have been rescaled for ease of comparison. Rotating away from $\theta_c = 0^\circ$, H_m initially rises before then decreasing to lower values of H around $\theta_c \approx 30^\circ$. (c) H_m versus θ_c for $\phi_a = \{12^\circ, 14^\circ, 18^\circ\}$. Open points are symmetrized from the solid measured points for $\phi_a = \{12^\circ, 14^\circ\}$. Error bars are determined as the standard deviation of a Gaussian fit to $\partial f/\partial H$. The slight asymmetry in $\pm\theta_c$ for $\phi_a = 18^\circ$ is likely indicative of a small misalignment of the sample of $\sim 1^\circ$. However, within error the profile for the $\phi_a = 18^\circ$ data either side of $\theta_c = 0^\circ$ broadly agrees very well, exhibiting a clear non-monotonic profile whereby H_m initially rises as θ_c is tilted away from 0° , before decreasing to a global minimum around $|\theta_c| = 36^\circ$. The inset illustrates the angular coordinate system we use throughout this work, as defined by Eqn. 1.

rises monotonically for increasing angular inclination of \mathbf{H} away from b [4]. Throughout the present study, we will adopt a convention of spherical polar coordinates in which the azimuthal angle ϕ_a is defined to be the inclination from b towards a , while the polar angle θ_c is the inclination out of the $b - a$ plane towards the c -axis. The magnetic field components oriented along each of the three Cartesian crystallographic axes are therefore related to these polar and azimuthal inclinations by the following expressions:

$$\begin{aligned} H_a &= H \cos \theta_c \sin \phi_a \\ H_b &= H \cos \theta_c \cos \phi_a \\ H_c &= H \sin \theta_c. \end{aligned} \quad (1)$$

Previous studies rotating \mathbf{H} in the $b - c$ plane have reported that the evolution of H_m appears to follow a $1/\cos \theta_c$ dependence [4, 5, 10]. Similarly, for nonzero values

of both ϕ_a and θ_c , measurements of the metamagnetic transition have discerned a monotonically rising profile of H_m upon increasing either θ_c or ϕ_a [11].

Methods – Contactless magnetoconductance measurements in pulsed magnetic fields were acquired by the proximity detector oscillator (PDO) technique [24]. A sample was mounted on a hand-wound planar coil with 6 turns possessing a diameter approximately matching the length of the sample (to maximize filling factor), with one outermost counter-winding added at a radius calculated to enclose the same amount of magnetic flux as the inner coil (but with opposite polarity). Note that throughout we invert Δf so that increasing f corresponds to increasing sample resistance. The PDO circuit rang at a frequency of 32 MHz, which was then mixed down twice to ~ 1 MHz and acquired using a JYTEK PXIe-69834 data acquisition card sampling at a rate of 30 megasamples

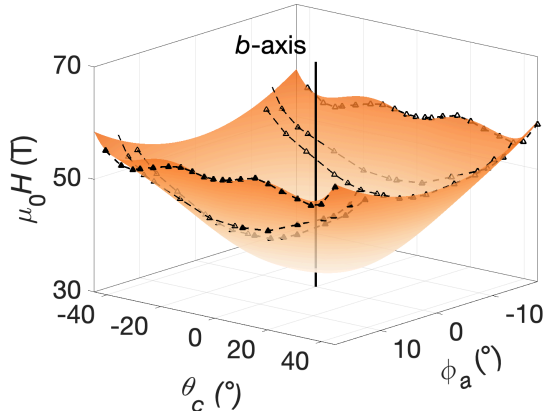


FIG. 2. Ripples in the metamagnetic transition surface of UTe_2 . Points are reproduced from Fig. 1c and plotted here in the three dimensions of H , θ_c and ϕ_a . The orange surface illustrates the profile of the first-order metamagnetic phase boundary, as measured at a temperature of 1.7 K. For sufficiently high H and ϕ_a the evolution of H_m with θ_c is highly non-monotonic.

per second. All data presented in this study were taken on the downsweep of the magnetic field pulse, which has a slower rate of change of H with time. All error bars are calculated from the standard deviation of Gaussian fitting to the first derivative of the PDO signal with respect to H .

Orienting \mathbf{H} at nonzero values of ϕ_a and θ_c was achieved by first mounting the PDO coil baseplate atop a small wedge of G10 machined to a desired azimuthal inclination. By rotating the relative orientation of \mathbf{H} through the plane orthogonal to the inclination of the G10 wedge, the polar angle θ_c could therefore be varied at a constant azimuthal inclination of ϕ_a . The sample was oriented on the PDO baseplate by Laue diffractometry, similar to refs. [8, 25]. All data were taken on the same sample, grown by the molten salt flux technique [26] following the methodology outlined in ref. [27], with a resistive T_c (in ambient H) of 2.09 K and a residual resistivity ratio of ~ 400 .

Results – Here we report measurements of the evolution of H_m in pulsed magnetic fields up to 57 T for rotations through θ_c at fixed values of ϕ_a . Figure 1 shows the contactless conductivity of UTe_2 measured by the PDO technique at incremental θ_c for $\phi_a = 18^\circ$. The metamagnetic transition manifests in the PDO signal as a sharp step in the PDO frequency as H_m is crossed. Fig. 1b identifies the location of H_m for each curve as the maximum of the derivative of the signal. The location of H_m for $\phi_a = 18^\circ$ clearly exhibits a non-monotonic dependence on θ_c . This is in contrast to the behavior observed for $\phi_a = 14^\circ$ and $\phi_a = 12^\circ$ (Fig. 1c), both of which continuously increase upon tilting θ_c towards 90° ; that being said, there does appear to be a slight inflection around $\theta_c \approx 25^\circ$ in the $\phi_a = 14^\circ$ dataset. Notably, for

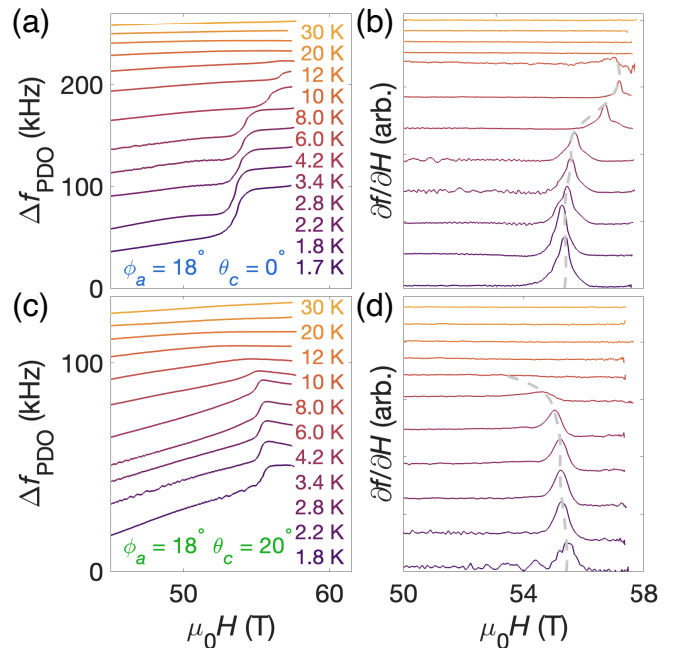


FIG. 3. Tracking the temperature dependence of H_m . (a) Contactless conductivity data measured by the PDO technique at incremental temperatures for \mathbf{H} aligned at $\phi_a = 18^\circ$, $\theta_c = 0^\circ$, with (b) the corresponding derivatives. (c) PDO measurements for \mathbf{H} tilted at $\phi_a = 18^\circ$, $\theta_c = 20^\circ$, with (d) the corresponding derivatives (again, derivative curves have been rescaled for ease of comparison). Whereas the location of H_m for the $\theta_c = 20^\circ$ dataset monotonically decreases with elevated temperature, by comparison at $\theta_c = 0^\circ$ H_m initially rises upon heating, before subsequently decreasing.

$\phi_a = 18^\circ$ we find that $H_m(\theta_c = 36^\circ) < H_m(\theta_c = 0^\circ)$, with $\mu_0 H_m(\theta_c = 36^\circ) = 53(1)$ T while $\mu_0 H_m(\theta_c = 0^\circ) = 54.6(8)$ T.

In Figure 2 we replot the data from Fig. 1c – namely, the locations of H_m determined from rotations of \mathbf{H} through θ_c at fixed $\phi_a = \{12^\circ, 14^\circ, 18^\circ\}$ – this time in the three-dimensional space of H , θ_c and ϕ_a . The b -axis is identified as the solid black line at $\theta_c = \phi_a = 0^\circ$. The metamagnetic transition surface is drawn in orange, which for sufficiently large H and ϕ_a exhibits a distinct ripple-like profile.

We track the evolution of $H_m(T)$ for two different angular orientations in Figure 3. For \mathbf{H} oriented at the inclination of $\phi_a = 18^\circ$, $\theta_c = 20^\circ$ the location of H_m – as identified by the sharp peak in $\partial f/\partial H$ at low T – gradually decreases with increasing H , and beyond the critical end point of the first-order transition it evolves into a broad crossover. This behavior is consistent with numerous other reports that also studied the evolution in temperature of polarized paramagnetism at high- H in UTe_2 [4, 12, 20, 21, 28, 29].

By contrast, for \mathbf{H} aligned such that $\phi_a = 18^\circ$, $\theta_c = 0^\circ$ – at the local minimum of the ripple in $H_m(\theta_c)$ in Fig. 1c – a markedly different behavior is exhibited. At

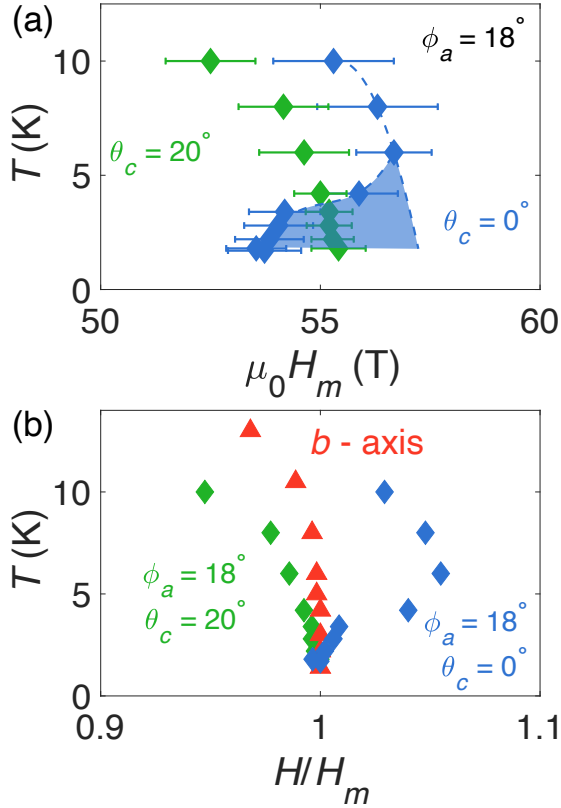


FIG. 4. Anomalous temperature evolution of metamagnetism. (a) The values of H_m extracted from the $\partial f/\partial H$ curves in Fig. 3 for $\theta_c = 20^\circ$ (green) and $\theta_c = 0^\circ$ (blue). (b) Normalized H/H_m for the points in panel (a) plotted alongside data for $\mathbf{H} \parallel b$ taken from ref. [20]. Whereas the $\phi_a = 18^\circ$, $\theta_c = 20^\circ$ (green) and $\phi_a = \theta_c = 0^\circ$ (orange) points monotonically decrease as the temperature is raised, the $\phi_a = 18^\circ$, $\theta_c = 0^\circ$ (blue) points anomalously increase, reaching a maximum around 6.0 K, before subsequently decreasing at higher T .

$T = 1.7$ K, $\mu_0 H_m = 53.7(8)$ T. H_m then *increases* upon raising T , to a maximal value of $\mu_0 H_m = 56.7(9)$ T at 6.0 K. At higher T , H_m then decreases, and the profile of the metamagnetic transition evolves into the broad crossover also observed at other inclinations of \mathbf{H} .

The anomalous profile of $H_m(T)$ for $\phi_a = 18^\circ$, $\theta_c = 0^\circ$ is particularly prominent when plotted alongside the normalized locations of H_m for other orientations of \mathbf{H} (Fig. 4b). While $H_m(\phi_a = 18^\circ, \theta_c = 20^\circ)$ and $H_m(\phi_a = \theta_c = 0^\circ)$ decrease smoothly and monotonically on raising T , $H_m(\phi_a = 18^\circ, \theta_c = 0^\circ)$ behaves quite differently. Firstly H_m rises gradually as T is incremented from 1.7 K to 3.4 K, and then rapidly increases around 4 K, reaching its maximum at 6.0 K. At higher T it appears to follow the same trend of other angular orientations, whereby the metamagnetic transition broadens and migrates down towards zero field.

To describe the metamagnetic transition in UTe_2 the-

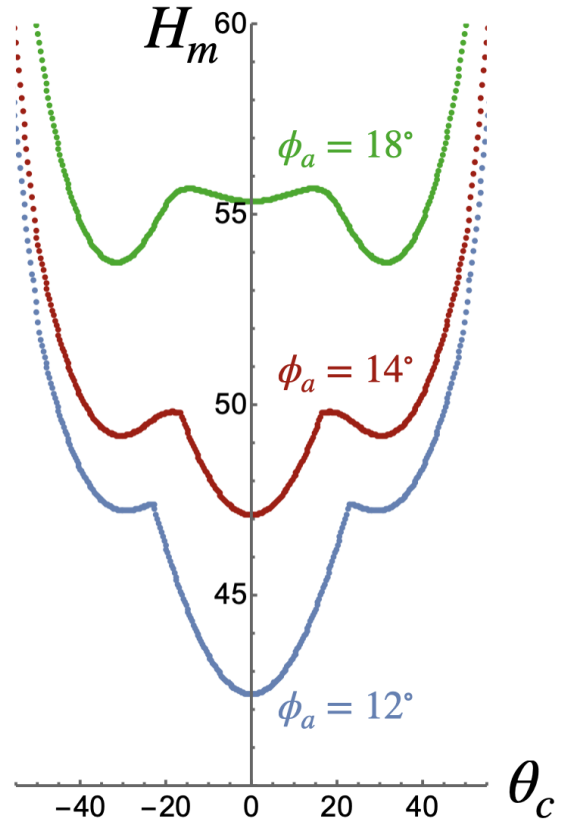


FIG. 5. Theoretically computed H_m versus θ_c for $\phi_a = \{12^\circ, 14^\circ, 18^\circ\}$ obtained by minimizing the Landau free energy of Eq. 2. We find good qualitative agreement with the experimental result presented in Fig. 1c.

oretically, we use the Landau free energy [8, 12, 30]

$$\mathcal{F} = \frac{\chi_i^{-1}}{2} M_i^2 + \frac{\beta_{ij}}{4} M_i^2 M_j^2 + \frac{\delta_{ijk}}{6} M_i^2 M_j^2 M_k^2 - \mathbf{M} \cdot \mathbf{H}, \quad (2)$$

where $i, j, k = a, b, c$ are spatial indices and parameters χ_i^{-1} , β_{ij} , and δ_{ijk} determine the metamagnetic phase transition, which occurs when a non-trivial minimum of the free energy becomes a global minimum once $H > H_m$. We find a range of parameters for which the calculated metamagnetic transition lines in Fig. 5 closely resemble the measured transition lines shown in Fig. 1. We note that the appearance of the ripples seems to be due to a proximity to an additional non-trivial local minimum in the free energy (Eqn. 2), which may lead to other observable effects that can be probed in future experiments, for example, those sensitive to fluctuations around this minimum.

Discussion – Our finding of non-monotonic H and T dependencies of metamagnetism in UTe_2 underscores the complexity of this material's high- H phase diagram. In our previous work [8] we proposed that for $H < H_m$, the superconductive state that persists up to $\mu_0 H \approx 35$ T for \mathbf{H} aligned close to b is likely mediated by ferromagnetic-

like fluctuations in the vicinity of H_m . Evidence favoring this scenario stems from the sensitivity to disorder of the angular extent of this superconducting phase [8], along with indirect measurements of the magnetic fluctuations from a magnetic entropy analysis [31], the findings of which concur with those from recent NMR experiments – a directly sensitive probe of the local spin susceptibility [17, 18, 32]. Notably, these NMR studies have observed a rotation of the local spin susceptibility from being predominantly along a at low H to aligning along b as H_m is approached, as one may expect for the scenario of triplet superconductivity mediated by ferromagnetic-like fluctuations in the vicinity of H_m .

However, the findings of the present study underline how little we understand about the microscopic properties of the polarized paramagnetic phase itself. A key challenge in studying UTe₂'s polarized paramagnetism lies in the necessity to access magnetic fields in excess of 35 T, precluding any scattering studies utilizing e.g. x-rays or neutrons that could map collective modes of magnetic excitations. Extraction magnetometry measurements in pulsed fields [21, 28] have indicated that H_m for $\mathbf{H} \parallel b$ is characterized by a sudden increase in the bulk magnetization of the material by an amount $\approx 0.5 \mu_B$ per unit cell (where μ_B is the Bohr magneton). A simple interpretation of this would be to assume that the polarized paramagnetic state is essentially ferromagnetic-like in character, with localized moments aligned along b . However, our observation of ripples in the metamagnetic transition surface at high H , accompanied by an anomalous temperature evolution of H_m in the vicinity of these ripples, implies that the microscopic magnetic properties of UTe₂ at $H > H_m$ may be far more complex.

Beyond the zeroth-order scenario of ferromagnetic-like ordering, we speculate that the polarized paramagnet may instead exhibit some more complicated magnetic structure, for example ferrimagnetic or helimagnetic ordering. Such a scenario would not be inconsistent with the extraction magnetometry result of a sudden jump in the net magnetization (provided that, for some complex heli-ordering, the moments are canted in such a manner to yield an overall net magnetization). Furthermore, the anomalous temperature dependence of H_m we observed for \mathbf{H} tilted to an orientation of $\phi_a = 18^\circ$, $\theta_c = 0^\circ$ (Figs. 3 & 4) suggests that, rather than consisting of one single homogeneous phase as previously thought [4], perhaps the large region of the high- H phase diagram generally referred to as polarized paramagnetism actually comprises one or more magnetic sub-phases. Such sub-phases could in principle exhibit distinctly different temperature evolutions. One possibility could be a form of heli-magnetic ordering that is sensitive to the magnitude and orientation of \mathbf{H} , yielding a slight rotation of the magnetic structure as a function of \mathbf{H} and T , thereby giving the ripple-like structure and seemingly anomalous T dependence of H_m that we observed.

We note that the anomalous temperature dependence of H_m (Figs. 3 & 4) within the ripple in the metamag-

netic transition surface is located at high \mathbf{H} tilted in the $b - a$ plane, i.e. with zero H_c component ($\theta_c = 0^\circ$). For $\mu_0 H \gtrsim 40$ T, b is the easy magnetic direction in UTe₂, while c is the hard axis [21]. Should there indeed exist some complex magnetic structure – either within a homogenous field polarized state, or in tandem with one or more magnetic sub-phases spanning the phase landscape – this observed sensitivity of $H_m(T)$ to zero and nonzero components of \mathbf{H} along the hard c direction perhaps provides a clue as to what the underlying high- H magnetic structure may be.

In summary, we mapped the metamagnetic transition surface of UTe₂ for rotations of \mathbf{H} through the polar angle θ_c at fixed azimuthal inclinations of ϕ_a . We observed a ripple-like non-monotonic dependence of the metamagnetic transition field H_m on θ_c at high H and high ϕ_a . Within this ripple the melting of the metamagnetic transition follows an anomalous non-monotonic temperature profile upon warming. These findings indicate that the magnetic properties of the high- H polarized paramagnetic state in UTe₂ are considerably more complex than previously considered.

ACKNOWLEDGMENTS

We gratefully acknowledge stimulating discussions with Theo Weinberger and Alex Hickey. This project was supported by the EPSRC of the UK (grant no. EP/X011992/1). Crystal growth and characterization were performed in MGML (mgml.eu), which is supported within the program of Czech Research Infrastructures (project no. LM2023065). We acknowledge financial support by the Czech Science Foundation (GACR), project No. 22-22322S. The work at UW-Madison (D.S.) was financially supported by the National Science Foundation, Quantum Leap Challenge Institute for Hybrid Quantum Architectures and Networks Grant No. OMA-2016136. D.V.C. acknowledges financial support from the National High Magnetic Field Laboratory through a Dirac Fellowship, which is funded by the National Science Foundation (Grant No. DMR-2128556) and the State of Florida. A.G.E. acknowledges support from Sidney Sussex College (University of Cambridge).

- [1] S. Ran, C. Eckberg, Q. P. Ding, Y. Furukawa, T. Metz, S. R. Saha, I. L. Liu, M. Zic, H. Kim, J. Paglione, and N. P. Butch, Nearly ferromagnetic spin-triplet superconductivity, *Science* **365**, 684 (2019).
- [2] D. Aoki, J. P. Brison, J. Flouquet, K. Ishida, G. Knebel, Y. Tokunaga, and Y. Yanase, Unconventional superconductivity in UTe_2 , *J. Phys. Condens. Matter* **34**, 243002 (2022).
- [3] V. Hutanu, H. Deng, S. Ran, W. T. Fuhrman, H. Thoma, and N. P. Butch, Low-temperature crystal structure of the unconventional spin-triplet superconductor UTe_2 from single-crystal neutron diffraction, *Acta Crystallogr. B* **76**, 137 (2020).
- [4] S. K. Lewin, C. E. Frank, S. Ran, J. Paglione, and N. P. Butch, A Review of UTe_2 at High Magnetic Fields, *Rep. Prog. Phys.* (2023).
- [5] S. Ran, I. L. Liu, Y. S. Eo, D. J. Campbell, P. M. Neves, W. T. Fuhrman, S. R. Saha, C. Eckberg, H. Kim, D. Graf, F. Balakirev, J. Singleton, J. Paglione, and N. P. Butch, Extreme magnetic field-boosted superconductivity, *Nat. Phys.* **15**, 1250 (2019).
- [6] G. Knebel, W. Knafo, A. Pourret, Q. Niu, M. Vališka, D. Braithwaite, G. Lapertot, M. Nardone, A. Zitouni, S. Mishra, I. Sheikin, G. Seyfarth, J. P. Brison, D. Aoki, and J. Flouquet, Field-Reentrant Superconductivity Close to a Metamagnetic Transition in the Heavy-Fermion Superconductor UTe_2 , *J. Phys. Soc. Jpn.* **88**, 63707 (2019).
- [7] A. Rosuel, C. Marcenat, G. Knebel, T. Klein, A. Pourret, N. Marquardt, Q. Niu, S. Rousseau, A. Demuer, G. Seyfarth, G. Lapertot, D. Aoki, D. Braithwaite, J. Flouquet, and J. P. Brison, Field-Induced Tuning of the Pairing State in a Superconductor, *Phys. Rev. X* **13**, 011022 (2023).
- [8] Z. Wu, T. I. Weinberger, J. Chen, A. Cabala, D. V. Chichinadze, D. Shaffer, J. Pospíšil, J. Prokleška, T. Haidamak, G. Bastien, V. Sechovský, A. J. Hickey, M. J. Mancera-Ugarte, S. Benjamin, D. E. Graf, Y. Skourski, G. G. Lonzarich, M. Vališka, F. M. Grosche, and A. G. Eaton, Enhanced triplet superconductivity in next-generation ultraclean UTe_2 , *Proc. Natl. Acad. Sci. USA* **121**, e2403067121 (2024).
- [9] R. Schönemann, P. F. Rosa, S. M. Thomas, Y. Lai, D. N. Nguyen, J. Singleton, E. L. Brosha, R. D. McDonald, V. Zapf, B. Maiorov, *et al.*, Sudden adiabaticity signals reentrant bulk superconductivity in UTe_2 , *PNAS Nexus* **3**, pgad428 (2024).
- [10] T. Helm, M. Kimata, K. Sudo, A. Miyata, J. Stirnat, T. Förster, J. Hornung, M. König, I. Sheikin, A. Pourret, *et al.*, Field-induced compensation of magnetic exchange as the possible origin of reentrant superconductivity in UTe_2 , *Nat. Commun.* **15**, 37 (2024).
- [11] S. K. Lewin, P. Czajka, C. E. Frank, G. S. Salas, H. Yoon, Y. S. Eo, J. Paglione, A. H. Nevidomskyy, J. Singleton, and N. P. Butch, High-Field Superconducting Halo in UTe_2 (2024), [arXiv:2402.18564 \[cond-mat.supr-con\]](https://arxiv.org/abs/2402.18564).
- [12] Z. Wu, T. I. Weinberger, A. J. Hickey, D. V. Chichinadze, D. Shaffer, A. Cabala, H. Chen, M. Long, T. J. Brumm, W. Xie, Y. Lin, Y. Skourski, Z. Zengwei, D. E. Graf, V. Sechovsky, G. G. Lonzarich, M. Vališka, F. M. Grosche, and A. G. Eaton, A quantum critical line bounds the high field metamagnetic transition surface in UTe_2 (2024), [arXiv:2403.02535 \[cond-mat.supr-con\]](https://arxiv.org/abs/2403.02535).
- [13] Z. Wu, H. Chen, T. I. Weinberger, A. Cabala, D. E. Graf, Y. Skourski, W. Xie, Y. Ling, Z. Zhu, V. Sechovský, M. Vališka, F. M. Grosche, and A. G. Eaton, Superconducting critical temperature elevated by intense magnetic fields, *Proc. Natl. Acad. Sci. USA* **122**, e2422156122 (2025).
- [14] B. Chandrasekhar, A note on the maximum critical field of high-field superconductors, *Appl. Phys. Lett.* **1**, 7 (1962).
- [15] A. M. Clogston, Upper Limit for the Critical Field in Hard Superconductors, *Phys. Rev. Lett.* **9**, 266 (1962).
- [16] H. Matsumura, H. Fujibayashi, K. Kinjo, S. Kitagawa, K. Ishida, Y. Tokunaga, H. Sakai, S. Kambe, A. Nakamura, Y. Shimizu, *et al.*, Large Reduction in the a -axis Knight Shift on UTe_2 with $T_c = 2.1$ K, *J. Phys. Soc. Jpn.* **92**, 063701 (2023).
- [17] K. Kinjo, H. Fujibayashi, S. Kitagawa, K. Ishida, Y. Tokunaga, H. Sakai, S. Kambe, A. Nakamura, Y. Shimizu, Y. Homma, D. X. Li, F. Honda, D. Aoki, K. Hiraki, M. Kimata, and T. Sasaki, Change of superconducting character in UTe_2 induced by magnetic field, *Phys. Rev. B* **107**, L060502 (2023).
- [18] Y. Tokunaga, H. Sakai, S. Kambe, P. Opletal, Y. Tokiwa, Y. Haga, S. Kitagawa, K. Ishida, D. Aoki, G. Knebel, G. Lapertot, S. Krämer, and M. Horvatić, Longitudinal Spin Fluctuations Driving Field-Reinforced Superconductivity in UTe_2 , *Phys. Rev. Lett.* **131**, 226503 (2023).
- [19] T. Vasina, D. Aoki, A. Miyake, G. Seyfarth, A. Pourret, C. Marcenat, M. Amano Patino, G. Lapertot, J. Flouquet, J.-P. Brison, D. Braithwaite, and G. Knebel, Connecting High-Field and High-Pressure Superconductivity in UTe_2 , *Phys. Rev. Lett.* **134**, 096501 (2025).
- [20] W. Knafo, M. Vališka, D. Braithwaite, G. Lapertot, G. Knebel, A. Pourret, J.-P. Brison, J. Flouquet, and D. Aoki, Magnetic-field-induced phenomena in the paramagnetic superconductor UTe_2 , *J. Phys. Soc. Jpn.* **88**, 063705 (2019).
- [21] A. Miyake, Y. Shimizu, Y. J. Sato, D. Li, A. Nakamura, Y. Homma, F. Honda, J. Flouquet, M. Tokunaga, and D. Aoki, Enhancement and Discontinuity of Effective Mass through the First-Order Metamagnetic Transition in UTe_2 , *J. Phys. Soc. Jpn.* **90**, 103702 (2021).
- [22] W. Knafo, M. Nardone, M. Vališka, A. Zitouni, G. Lapertot, D. Aoki, G. Knebel, and D. Braithwaite, Comparison of two superconducting phases induced by a magnetic field in UTe_2 , *Commun. Phys.* **4**, 40 (2021).
- [23] C. E. Frank, S. K. Lewin, G. Saucedo Salas, P. Czajka, I. M. Hayes, H. Yoon, T. Metz, J. Paglione, J. Singleton, and N. P. Butch, Orphan high field superconductivity in non-superconducting uranium ditelluride, *Nat. Commun.* **15**, 3378 (2024).
- [24] M. M. Altarawneh, C. H. Mielke, and J. S. Brooks, Proximity detector circuits: An alternative to tunnel diode oscillators for contactless measurements in pulsed magnetic field environments, *Rev. Sci. Instr.* **80**, 066104 (2009).
- [25] T. I. Weinberger, Z. Wu, D. E. Graf, Y. Skourski, A. Cabala, J. Pospíšil, J. Prokleška, T. Haidamak, G. Bastien, V. Sechovský, G. G. Lonzarich, M. Vališka, F. M. Grosche, and A. G. Eaton, Quantum Interference be-

- tween Quasi-2D Fermi Surface Sheets in UTe_2 , *Phys. Rev. Lett.* **132**, 266503 (2024).
- [26] H. Sakai, P. Opletal, Y. Tokiwa, E. Yamamoto, Y. Tokunaga, S. Kambe, and Y. Haga, Single crystal growth of superconducting UTe_2 by molten salt flux method, *Phys. Rev. Mater.* **6**, 073401 (2022).
- [27] A. G. Eaton, T. I. Weinberger, N. J. M. Popiel, Z. Wu, A. J. Hickey, A. Cabala, J. Pospíšil, J. Prokleška, T. Haidamak, G. Bastien, P. Opletal, H. Sakai, Y. Haga, R. Nowell, S. M. Benjamin, V. Sechovský, G. G. Lonzarich, F. M. Grosche, and M. Vališka, Quasi-2D Fermi surface in the anomalous superconductor UTe_2 , *Nat. Commun.* **15**, 223 (2024).
- [28] A. Miyake, Y. Shimizu, Y. J. Sato, D. Li, A. Nakamura, Y. Homma, F. Honda, J. Flouquet, M. Tokunaga, and D. Aoki, Metamagnetic Transition in Heavy Fermion Superconductor UTe_2 , *J. Phys. Soc. Jpn.* **88** (2019).
- [29] M. Vališka, T. Haidamak, A. Cabala, J. Pospíšil, G. Bastien, V. Sechovský, J. Prokleška, T. Yanagisawa, P. Opletal, H. Sakai, Y. Haga, A. Miyata, D. Gorbunov, and S. Zherlitsyn, Dramatic elastic response at the critical end point in UTe_2 , *Phys. Rev. Mater.* **8**, 094415 (2024).
- [30] H. Yamada, Metamagnetic transition and susceptibility maximum in an itinerant-electron system, *Phys. Rev. B* **47**, 11211 (1993).
- [31] Y. Tokiwa, P. Opletal, H. Sakai, S. Kambe, E. Yamamoto, M. Kimata, S. Awaji, T. Sasaki, D. Aoki, Y. Haga, and Y. Tokunaga, Reinforcement of superconductivity by quantum critical fluctuations of metamagnetism in UTe_2 , *Phys. Rev. B* **109**, L140502 (2024).
- [32] K. Kinjo, H. Fujibayashi, H. Matsumura, F. Hori, S. Kitagawa, K. Ishida, Y. Tokunaga, H. Sakai, S. Kambe, A. Nakamura, Y. Shimizu, Y. Homma, D. Li, F. Honda, and D. Aoki, Superconducting spin reorientation in spin-triplet multiple superconducting phases of UTe_2 , *Sci. Adv.* **9**, eadg2736 (2023).